Supporting Information for

Revealing the Electronic and Molecular Structure of Randomly Oriented Molecules by Polarized Two-photon Spectroscopy

Marcelo G. Vivas[1], Daniel L. Silva[2], Leonardo De Boni[1], Yann Bretonniere[3], Chantal Andraud[3], Florence Laibe-Darbour[4], J-C Mulatier[4], Robert Zaleśny[5], Wojciech Bartkowiak[5], Sylvio Canuto[2] and Cleber R. Mendonca[1]

[1]*Instituto de Física de São Carlos, Universidade de São Paulo, Caixa Postal 369, 13560-970 São Carlos, SP, Brazil*

[2]*Instituto de Física, Universidade de São Paulo, CP 66318, 05314-970, São Paulo, SP, Brazil*

[3]*CNRS, Université Lyon I, ENS-Lyon, 46 allée d'Itale, 69364 Lyon, France*

[4]*Laboratoire de Chimie, CNRS UR 5182, ENS de Lyon, Université Lyon I, 46 allée d'Italie, 69364Lyon cedex 07, France*

[5]*Theoretical Chemistry Group, Institute of Physical and Theoretical Chemistry, Wroclaw University of Technology, Wybrzeze Wyspianskiego 27, 50-370 Wroclaw, Poland*

Corresponding Authors: mavivas82@yahoo.com.br and crmendonca@ifsc.usp.br

Summary

SI.1 – Experimental procedures

All chemicals were of reagent grade and used as supplied (Sigma-Aldrich). The molecular structure of the chiral organic molecules (**FD43** and **FD48**) is presented in Fig. 1. As can be observed in Fig. 1, **FD43** presents molecular chirality because of the chiral carbon attached to the phenyl ligand, while the chirality of **FD48** is due to their helical molecular structure. Details about the synthesis and purification can be found in Ref [1].
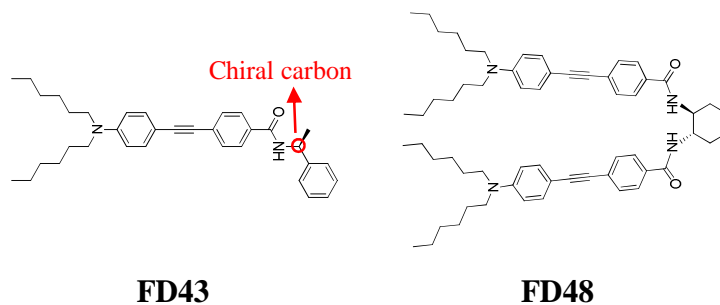

FD43   **FD48**

Figure SI.1 - Structures of the chiral molecules studied based on phenylacetylene (**FD43** and **FD48**).

We prepared **FD43** and **FD48** chloroform solution with concentrations 5×10^{16} and (approximately) 10^{18} molecules/cm^3, for linear and nonlinear optical measurements, respectively. For the spectroscopic measurements the sample was placed in a 2 mm thick quartz cuvette. The circular dichroism (CD) spectrum was recorded using a Jasco J-815 Spectrometer. Figure SI.2 displays the CD spectra for (a) **FD43** and (b) **FD48** molecules. The electronic circular dichroism is defined (cgs system of units) as the difference in the molar absorptivity for left circularly and right circularly polarized light, i.e.,

$$\Delta\varepsilon_{CD}\left(\omega\right) = \varepsilon_L - \varepsilon_R = \frac{64\pi^2 N_A \omega}{9\times10^3 \ln\left(10\right)\hbar c}\frac{L^2}{n}R^f\ g\left(\omega\right), \tag{S.1}$$

where $\hbar$ is Planck's constant divided by 2π, c is the speed of light, ω is the excitation laser frequency, $L = 3n^2/\left(2n^2+1\right)$ is the Onsager local field factor introduced to take into account the medium effect with [2] with $n=1.49$ for chloroform and $g\left(\omega\right)$ represents the linewidth function. R^f is the electronic circular dichroism strength, which is given the expression:

$$R^f = \frac{3}{4}\text{Im}\left(\vec{\mu}_{gf}\bullet\vec{m}_{gf}\right) \qquad (S.2)$$

and $\vec{\mu}_{gf}$ and $\vec{m}_{gf}$ are, respectively, the transition electric and magnetic dipole moments. The solid lines in Fig. SI.2 shows the fit of the lowest energy band using the Eq. S.1. Considering that the dipole moments are parallels we can estimate the magnetic dipole moment magnitude since $\vec{\mu}_{gf}$ can be obtained from the linear absorption spectrum [1].
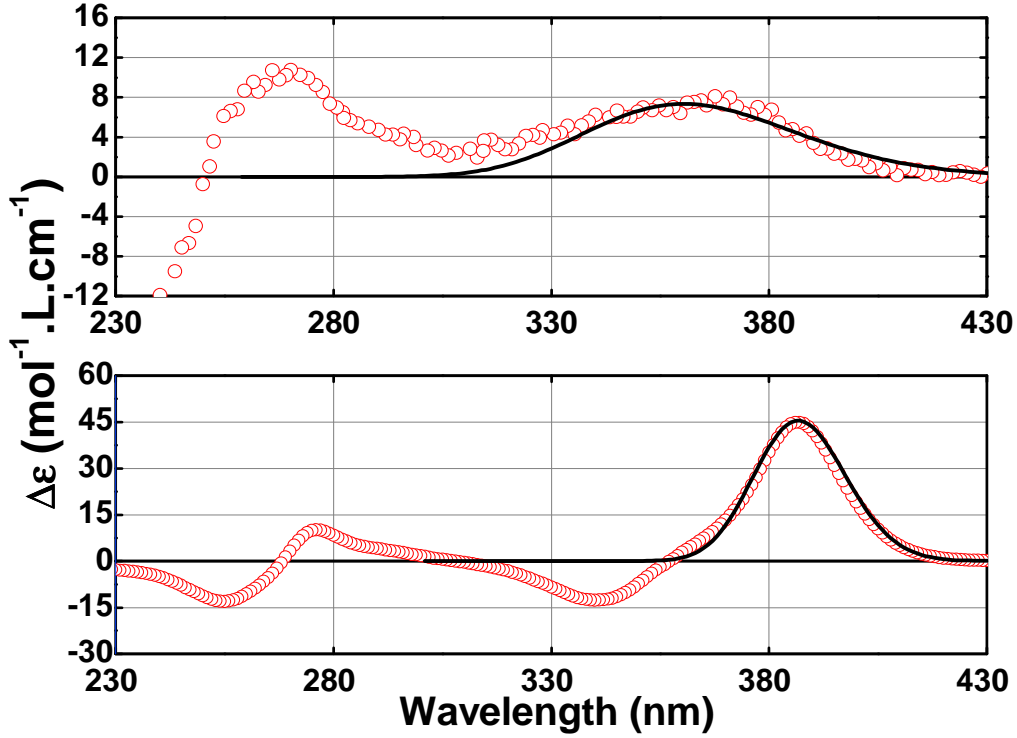

Figure SI.2 – CD spectra of **FD43** (top) and **FD48** (bottom) molecules.

For the nonlinear optical measurements, we employed the open aperture Z-scan technique, using 120-fs laser pulses from an optical parametric amplifier pumped by 150-fs pulses (775 nm) from a Ti:sapphire chirped pulse amplified system. The Z-scan measurements were carried out with intensities ranging from 100 to 200 GW/cm^2 (50 to 120 nJ/pulse) and with beam waist size at the focus varying from 15 to 18 μm. To ensure a Gaussian profile for the laser beam used in the experiments, spatial filtering is performed before the Z-scan setup. A silicon detector was employed to monitor the laser beam intensity in the far-field. To improve the signal to noise ratio, we employed the oscillatory Z-scan method, in which the sample is continuously scanned, repeating the experiment several times.

Moreover, we used a lock-in amplifier to integrate 1000 shots for each point of the Z-scan signature.

In the open aperture Z-scan technique, 2PA cross-section is determined by translating the sample through the focal plane of a focused Gaussian beam, while transmittance changes in the far field intensity are monitored. For a 2PA process, the light field creates an intensity dependent absorption, $\alpha = \alpha_0 + \beta I$; in which I is the laser beam intensity, α_0 is the linear absorption coefficient, and β is the 2PA coefficient. Far from one-photon resonances, the power transmitted through the sample, for each wavelength, is integrated over time (assuming a pulse with a Gaussian temporal profile) to give the normalized energy transmittance,

$$T(z) = \frac{1}{\sqrt{\pi} q_o(z,0)} \int_{-\infty}^{\infty} \ln\left[1 + q_o(z,0)e^{-\tau^2}\right] d\tau \qquad (S.3)$$

with

$$q_o = \beta I_o L \left(1 + \left(z^2/z_o^2\right)\right)^{-1} \qquad (S.4)$$

where L is the sample thickness, z_0 is the Rayleigh length, z is the sample position, and I_0 is the laser intensity at the focus. The nonlinear coefficient β is obtained by fitting the Z-scan data with Eq. (1). The 2PA cross-section, σ_{2PA}, is determined from $\sigma_{2PA} = \hbar\omega\beta/N$, where $\hbar\omega$ is the excitation photon energy, and N is the number of chromophores per cm^3. The 2PA cross-section is expressed in Göppert-Mayer units (GM), where $1\text{GM} = 1\times10^{-50}\text{cm}^4.\text{s.photon}^{-1}$.

To control the laser polarization state from linear to circular, we used a broadband zero-order quarter-wave plate. To guarantee the same experimental condition for the measurements, the quarter-wave plate is kept in the setup in both experiments (linear and circular polarization), i.e., we set the angle of rotation of the λ/4 wave plate at 0° for linear polarization and at 45° for circular polarization.

Since 2PA-CLD is a nonlinear optical effect that is governed by the electric dipole moment, the difference between the 2PA cross-sections using circularly and linearly polarized light is significantly large in most molecules. Therefore, the 2PA-CLD signal can be easily determined by employing the well-known open aperture Z-scan. In the present work the 2PA measurements using circularly and linearly polarized light were performed independently in separated runs. Afterward, the recovered 2PA cross-sections were combined according to the equation that defines 2PA-CLD ($\Delta\sigma_{CLD}^{2PA}(\lambda) = \left[\Omega_{CLD}^{2PA}(\lambda) - 1\right]\Big/\left[\Omega_{CLD}^{2PA}(\lambda) + 1\right]$

). Figure SI.3 shows typical open aperture Z scan curves measured using linearly polarized (LP) (circles) and circularly polarized (CP) (squares) light at three different wavelengths. The difference in TPA using CP and LP depends on the excitation wavelength.
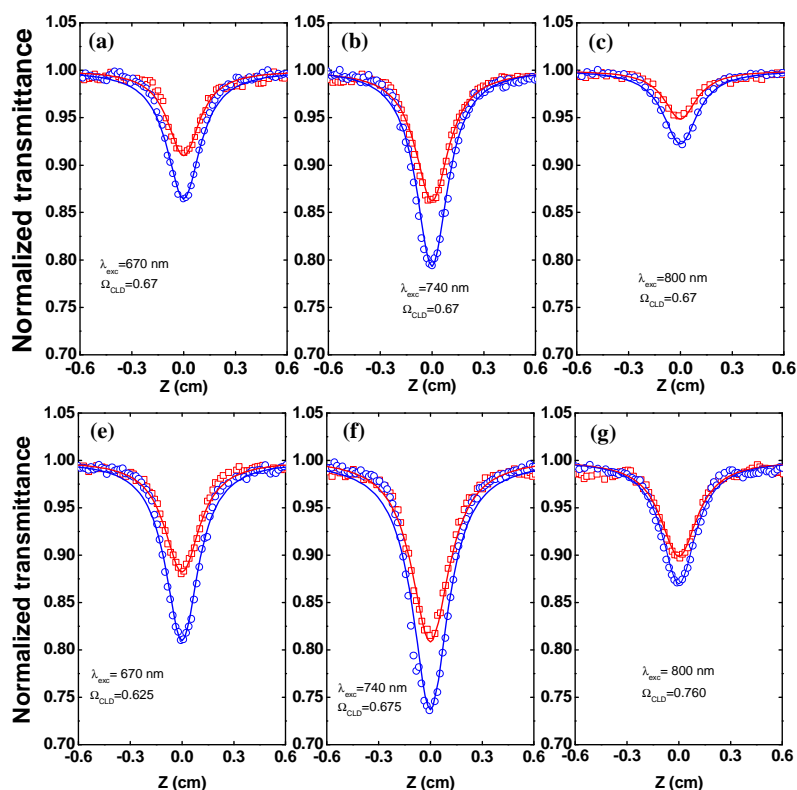

Figure SI.3 – Open-aperture Z-scan curves for **FD43** (a-c) and **FD48** (e-g) with linearly (circles), left (up triangles) and right (squares) circularly polarized light. The solid line represents the fitting employing the theory described in Ref. [3].

SI.2 – Computational details

In the present work all quantum-chemical calculations were performed using the Kohn-Sham formulation of density functional theory (KS-DFT). The equilibrium molecular geometries of the studied molecules were determined performing DFT calculations employing the hybrid exchange-correlation B3LYP [4,5] functional and the standard 6-311G(d,p) basis set [6] as implemented in the Gaussian 03 package.[7] In these calculations the molecules were assumed to be *in vacuo*. Subsequently, to determine the lowest one- and two-photon allowed states of the studied molecules, the response functions calculations within the DFT framework were performed using the DALTON program.[8] In this approach, the excitation energies and transition dipole moments (two-photon probabilities) are analytically computed as, respectively, poles and single residues of the linear (quadratic) response

function of the molecular electronic density. The excited states dipole moments were also determined in the present work by computing the double residue of the quadratic response function. Moreover, (electronic) circular dichroism (CD) calculations were also performed within the DFT framework using the DALTON program.[8] The rotatory strengths were calculated for the twenty lowest-energy transitions and the CD spectra of the studied molecules were simulated and compared with the experimental spectra. All the response functions and CD calculations were performed employing the hybrid exchange-correlation B3LYP [4,5] functional in combination with the standard 6-31+G(d) basis set [6] assuming the molecules *in vacuo*.

The orientationally averaged two-photon absorption probability ($\delta_{0f}^{2PA}(\omega_{0f})$) for the degenerate case is given by,[9]

$$\overline{\delta}_{gf}^{2PA}\left(\omega_{gf}\right)=\frac{1}{30}\sum_{\alpha\beta}\left(F\times S_{\alpha\alpha}^{gf}S_{\beta\beta}^{*,gf}+G\times S_{\alpha\beta}^{gf}S_{\alpha\beta}^{*,gf}+H\times S_{\alpha\beta}^{gf}S_{\beta\alpha}^{*,gf}\right),\tag{S.5}$$

where the two-photon transition takes place from the ground state $\left|g\right\rangle$ to a final excited state $\left|f\right\rangle$. The $\alpha\beta$ element of the two-photon tensor $S_{\alpha\beta}^{gf}$ depends on the light angular frequency ω ($\omega=\omega_{gf}/2$) and, F, G and H are scalars used to define the polarization of light (F = G = H = 2 for LP and F = -2, G = 3 and H = 3 for CP). Because of the symmetry of the two-photon tensor, Eq. (S.5) simplifies to [9]

$$\overline{\delta}_{gf}^{2PA}\left(\omega_{gf}\right)=FA\left(\omega_{gf}\right)+\left(G+H\right)B\left(\omega_{gf}\right),\tag{S.6}$$

where $A\left(\omega_{gf}\right)=\dfrac{1}{30}\sum_{\alpha\beta}S_{\alpha\alpha}^{gf}S_{\beta\beta}^{*,gf}$ and $B\left(\omega_{gf}\right)=\dfrac{1}{30}\sum_{\alpha\beta}S_{\alpha\beta}^{gf}S_{\alpha\beta}^{*,gf}$. $\overline{\delta}_{gf}^{2PA}\left(\omega_{gf}\right)$ is given in atomic units.

The simulated 2PA cross-section spectra for both LP and CP were obtained using Eq. S.7, [10,11]

$$\sigma_{gf}^{2PA}(2\omega)=\frac{4\pi^{3}\alpha a_{0}^{5}}{c}\sum_{f=1}^{n}\left[(\hbar\omega_{gf}/2)^{2}\overline{\delta}_{gf}^{2PA}(\omega_{gf})g(2\omega,\omega_{gf},\Gamma)\right]\tag{S.7}$$

where α is the fine structure constant, a_0 is the Bohr's radium, c is the speed of light and $E_{gf}=\hbar\omega_{gf}/2$ is the photon energy (half of the transition energy). $g\left(2\omega,\omega_{gf},\Gamma\right)$ represents the line-shape function of the final excited state. Here we have used a Lorentzian function given by

$$g(2\omega, \omega_{gf}, \Gamma) = \frac{1}{\pi} \frac{\Gamma_{gf}}{(\omega_{gf} - 2\omega)^2 + \Gamma_{gf}^2} \qquad \text{(S.8)}$$

where Γ (in s^{-1}) is the damping constant described as the half width at half-maximum (HWHM) of the final excited state line-width. To simulate the 2PA spectra, in this report it was adopted $\Gamma = 0.2$ eV ($\sim 0.5 \times 10^{14}$ s^{-1} or $\sim 0.75 \times 10^{-2}$ atomic units) for all 2PA electronic transitions playing along the spectral UV-Vis region. This specific value was estimated from the experimental 2PA spectra. To obtain the 2PA cross-sections in Göppert–Mayer units, in Eq. (S.7) one has to use $a_0 = 5.291772108 \times 10^{-9}$ cm, $c = 2.99792458 \times 10^{10}$ cm/s and the values of $E = \hbar\omega_{gf}/2$, Γ and $\bar{\delta}_{gf}^{2PA}(\omega_{gf})$ in atomic units.

Table S.1 – Summary of the theoretical results provided by the quadratic response function calculations performed within the DFT framework (B3LYP/6-31+G(d)). n is the excited state number; $A(\omega_{gf})$ (a.u.) and $B(\omega_{gf})$ (a.u.) are molecular parameters; $\sigma_{gf,LP}^{2PA}(\omega_{gf})$ (GM) and $\sigma_{gf,CP}^{2PA}(\omega_{gf})$ (GM) are the 2PA cross-sections for LP and CP, respectively and $\Omega_{CLD}^{2PA} = \sigma_{gf,CP}^{2PA}(\omega_{gf})/\sigma_{gf,LP}^{2PA}(\omega_{gf})$ is the ratio between the 2PA cross-sections obtained using CP and LP.

n	λ (nm)	$A(\omega_{gf})$ (a.u.)	$B(\omega_{gf})$ (a.u.)	$\sigma_{gf,LP}^{2PA}(\omega_{0f})$ (GM)	$\sigma_{gf,CP}^{2PA}(\omega_{gf})$ (GM)	Ω_{CLD}^{2PA}
FD43						
S_1	379	12100	12300	144	97	0.676
S_5	286	11000	9980	213	130	0.612
S_8	275	7070	7470	164	114	0.697
FD48						
n	λ (nm)	$A(\omega_{gf})$ (a.u.)	$B(\omega_{gf})$ (a.u.)	$\sigma_{gf,LP}^{2PA}(\omega_{0f})$ (GM)	$\sigma_{gf,CP}^{2PA}(\omega_{gf})$ (GM)	Ω_{CLD}^{2PA}
S_2	384	6510	10100	102	91	0.891
S_3	361	11200	7110	110	44	0.399
S_{16}	280	9350	12900	253	211	0.835
S_{19}	274	19500	14000	357	169	0.474

By merging the 2PA-CLD definition with Eqs. (S.6) and (S.7), one can obtain the following simple expression for the theoretical 2PA-CLD spectra written in terms of $A(\omega_{gf})$ and $B(\omega_{gf})$,[12-15]

$$\Delta\sigma^{2PA-CLD}\left(2\omega\right)=\frac{\sum_{f}g\left(2\omega,\omega_{gf},\Gamma\right)\cdot\left(-2A\left(\omega_{gf}\right)+B\left(\omega_{gf}\right)\right)}{\sum_{f}g\left(2\omega,\omega_{gf},\Gamma\right)\cdot\left(5B\left(\omega_{gf}\right)\right)},$$

(4)

(S.9)

To simulate the CD spectra, the same linewidths used to simulate the 2PA spectra were also adopted for the transitions playing along the investigated spectral region. The simulated CD spectra are presented in Fig. SI.4
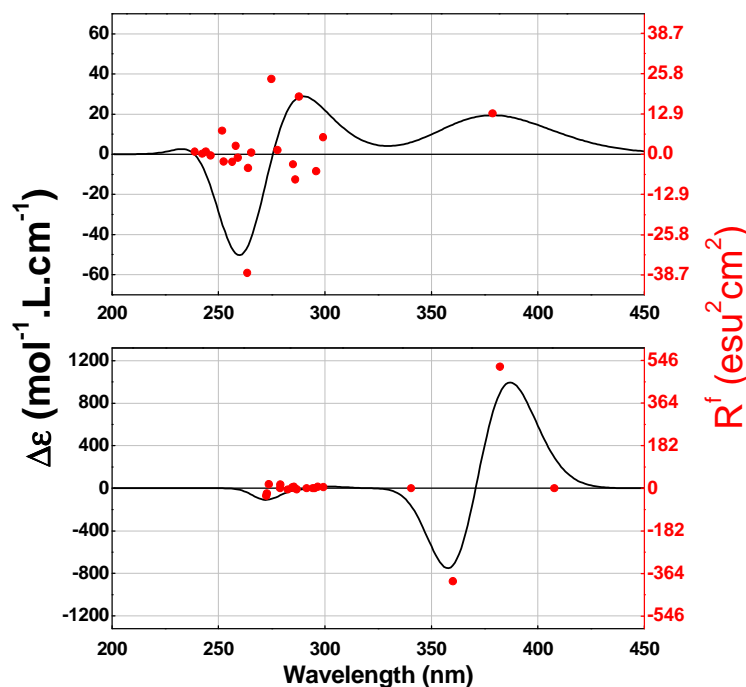

Figure SI.4 – (a) Simulated CD spectrum of **FD43** (top) and **FD48** (bottom) molecules.

From a comparison between experimental and simulated CD spectra (Figs. SI.2 and SI.4) one can note that the CD calculations provided results consistent with the experimental data. For both molecules the simulated CD spectra reproduce the shape of the experimental spectra. The good agreement between simulated and experimental CD spectra evidences that the equilibrium molecular geometries determined through DFT calculations assuming **FD43** and **FD48** *in vacuo* are adequate to study their spectroscopic properties in solvents with low dielectric constant, such as chloroform. The theoretical values for $\Delta\varepsilon_{CD}$ and R^{f} are certainly overestimated, nevertheless from a comparison between the theoretical values determined for **FD43** and **FD48** becomes evident the larger chirality of **FD48** molecule, as it was experimentally verified.

SI.3 – Sum-over-essential states approach: Two-photon circular-linear dichroism

Two-photon circular-linear dichroism (2PA-CLD) is a nonlinear optical effect governed by the electric transition dipole moment. Consequently, 2PA-CLD is a third-order nonlinear optical effect governed by the electric dipole moment, therefore much more intense than the 2PA-CD, opening access to the determination of the angle between electric transition dipole moments and the symmetry of excited states of achiral samples. Moreover, since right and left circular polarization are identical within the electric dipole approximation, one can use either one in non-optically active samples. 2PA-CLD was firstly proposed by Wanapun et. al. [15] in 2006 and can be expressed as:

$$\Delta\sigma_{CLD}^{2PA}(\omega) = \frac{\Omega_{CLD}^{2PA}(\omega)-1}{\Omega_{CLD}^{2PA}(\omega)+1},$$

(S.10)

where $\Omega_{CLD}^{2PA}(\omega) = \sigma_{CP}^{2PA}(\omega)/\sigma_{LP}^{2PA}(\omega)$ is the ratio between the 2PA cross-section obtained using circularly ($\sigma_{CP}^{2PA}(\omega)$) and linearly ($\sigma_{LP}^{2PA}(\omega)$) polarized light.

According to the second order time-dependent perturbation theory the 2PA cross-section can be evaluated, in the cgs system of units, as [16]:

$$\sigma_{2PA}(2\omega) = 2\frac{(2\pi)^5}{(nhc)^2}\omega^2 L^4 \sum_{\alpha\beta}\left|S_{\alpha\beta}^{gf}(\omega)\right|^2 g_{gf}(2\omega,\omega_{gf},\Gamma),$$

(S.11)

where h is Planck's constant, c is the speed of light, ω is the excitation laser frequency, $L = 3n^2/(2n^2+1)$ is the Onsager local field factor introduced to take into account the effect media [2] with $n=1.49$ for chloroform and $g(2\omega)$ represents the linewidth function. $S_{\alpha\beta}^{gf}(\omega)$ is the 2PA transition matrix elements given by:

$$S_{\alpha\beta}^{gf}(\omega) = \sum_{k=0,1,2,...N}\frac{\langle f|\vec{\mu}_{\alpha\beta}\bullet\hat{e}|k\rangle\langle k|\vec{\mu}_{\alpha\beta}\bullet\hat{e}|g\rangle}{(\omega_{gk}-\omega)-i\Gamma_{gk}(\omega)}$$

(S.12)

where $\vec{\mu}$ is the dipole moment vector, Γ_{gk} is the damping constant describing HWHM of the final state linewidth (assuming Lorentzian line-shape), ω_{gf} is the transition frequency, $\hat{e}$ is the versor that describes the light polarization state and the subscripts α and β represent the

Cartesian indices. The summation represents the sum-over-all real electronic states, i.e., the initial ($|g\rangle$), intermediate ($|m\rangle$) and final ($|f\rangle$) states.

Many molecules, including those studied here, do not present a center of inversion and, therefore, initial and final states have permanent dipole moment. In addition, in non-centrosymmetric molecules the electric dipole selection rule are most likely relaxed [17] and, therefore, one- and two-photon transitions are allowed between any electronic states. For a non-centrosymmetric molecule as the **FD43** the 2PA cross-section can be estimated by using a two-level system model (Fig. SI.5 (a)) and taking into account the average over all possible molecular orientations in an isotropic medium, as:

$$\sigma_{01}^{2PA}(2\omega) = \frac{2(2\pi)^5}{(nhc)^2}\omega^2 L^4 \left[\left[\sum_{\alpha\beta}\frac{\left(\hat{e}\bullet\vec{\mu}_{01}^{\alpha\beta}\right)\left(\Delta\vec{\mu}_{01}^{\alpha\beta}\bullet\hat{e}\right)}{\omega}\right]\right]^2 g_{01}(2\omega), \tag{S.13}$$

As it can be observed in Eq. S.13 the 2PA cross-section depends on the light polarization state. In an anisotropic medium like a solution, where the molecule is randomly oriented with respect to polarization of the excitation beam, it is necessary to take into account the orientational average on all the possible directions of the molecular dipole moment. For this, it is necessary to employ the Euler Integral [18] having as integrand the 2PA transition matrix element. Proceeding in this way, we have:

$$\left\langle\sigma_{01}^{(2PA)}(\theta,\psi,\phi)\right\rangle = \frac{2(2\pi)^5}{(nhc)^2}L^4 g_{01}(2\omega)\left\langle\left|S_{01}^{(2PA)}(\theta,\psi,\phi)\right|^2\right\rangle = \tag{S.14}$$

$$\frac{2(2\pi)^5}{(nhc)^2}L^4 g_{01}(2\omega)\frac{1}{8\pi^2}\int\limits_0^{2\pi}d\phi\int\limits_0^{2\pi}d\psi\int\limits_0^{\pi}sen(\theta)\sum_{\alpha\beta}\left(\hat{e}\bullet\vec{\mu}_{01}^{\alpha\beta}\right)\left(\vec{\mu}_{01}^{\alpha\beta}\bullet\hat{e}\right)^*\left(\Delta\vec{\mu}_{01}^{\alpha\beta}\bullet\hat{e}\right)\left(\hat{e}\bullet\Delta\vec{\mu}_{01}^{\alpha\beta}\right)^* d\theta$$

where (θ,ψ,ϕ) are the Euler angles.

Considering the linearly and circularly polarized beam and the methodology described by Andrews and Thirunamachandran [19,20], the Eq. (S.14) provides the following equation in a two-energy level model in non-centrosymmetric molecules [21]:

$$\sigma_{g\rightarrow f}^{(2PA)}(\omega) = \frac{2}{30}\frac{(2\pi)^5}{(nhc)^2}L^4 P\left(\theta_{\vec{\mu}_{01}\Delta\vec{\mu}_{01}}\right)\left|\vec{\mu}_{01}\right|^2\left|\Delta\vec{\mu}_{01}\right|^2 g_{01}(2\omega) \tag{S.15}$$

In Eq. (S.15), $P(\theta)$ describes the polarization light state, being

$$\eta = P_L\left(\theta_{\bar{\mu}_{01}\Delta\bar{\mu}_{01}}\right) = 2\left(2\cos^2\left(\theta_{\bar{\mu}_{01}\Delta\bar{\mu}_{01}}\right)+1\right), \tag{S.16}$$

for **linear polarization** and

$$\tau = P_C\left(\theta_{\bar{\mu}_{01}\Delta\bar{\mu}_{01}}\right) = \left(\cos^2\left(\theta_{\bar{\mu}_{01}\Delta\bar{\mu}_{01}}\right)+3\right), \tag{S.17}$$

for **circular polarization.** θ is the angle between the dipole moments $\bar{\mu}_{01}$ and $\Delta\bar{\mu}_{01}$. Therefore, according to this approach, circular-linear ration can be written as: [21,22]

$$\Omega^{2PA}_{CLD} = \left\{ \frac{\cos^2\left(\theta_{\bar{\mu}_{01}\Delta\bar{\mu}_{01}}\right)+3}{2\left[2\cos^2\left(\theta_{\bar{\mu}_{01}\Delta\bar{\mu}_{01}}\right)+1\right]} \right\}. \tag{S.18}$$
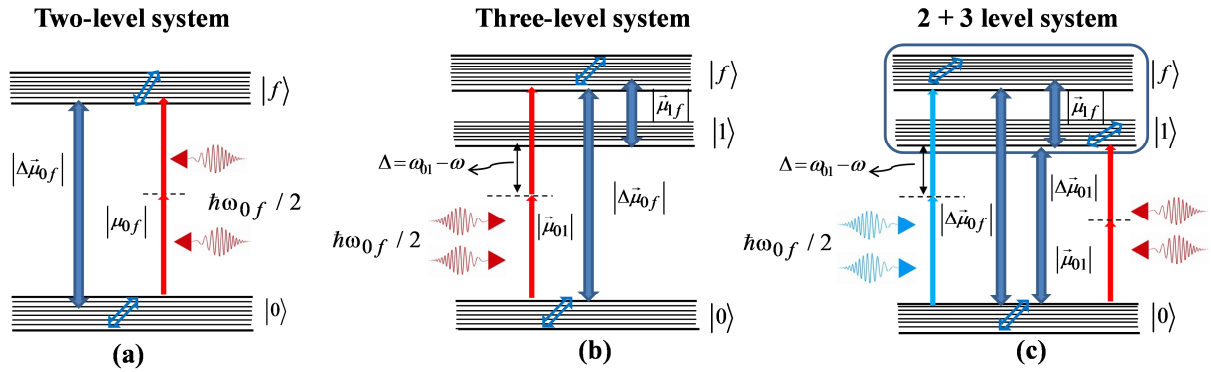

Figure SI.5 – (a) 2PA transition in a two-level system with a permanent dipole moment difference between ground and final excited state ($\Delta\bar{\mu}_{0f} \neq 0$). (b) 2PA transitions in a three-energy level system. There are two distinct transition pathways for 2PA in this system. The first path involves the permanent dipole moment difference between ground and final excited state ($\Delta\bar{\mu}_{0f} \neq 0$), while the second involves the same initial and final states but with an intermediate one-photon resonance (blue arrows) due to the detuning between the photon energy and the first excited state allowed by 1PA. (c) 2PA transition in a 2 + 3 level system. Such system is a linear combination of the two diagrams previously described.

It is observed that in a two-level system the Ω^{2PA}_{CLD} signal varies between 0.667 and 1.5 for any value of angle between the dipole moments and does not depend on the wavelength. Therefore, using the 2PA cross-section obtained from the Z-scan technique it is possible to determine the angle between the dipole moments. Moreover, according to theoretical results reported by Nascimento, [22] on the polarization dependence of 2PA rates for randomly oriented molecules, $0 \leq \Omega^{2PA}_{CLD} < 1$ for $0^o \leq \theta_{\bar{\mu}_{01}\Delta\bar{\mu}_{01}} < 54.7^o$, $1 \leq \Omega^{2PA}_{CLD} < 1.5$ for $54.7^o \leq \theta_{\bar{\mu}_{01}\Delta\bar{\mu}_{01}} < 90^o$, and $\Omega^{2PA}_{CLD} = 1.5$ for $\theta_{\bar{\mu}_{01}\Delta\bar{\mu}_{01}} = 90^0$. Nascimento also showed that

$\theta_{\bar{\mu}_{01}\bar{\mu}_{1f_i}} = 90^o$ corresponds to transitions between states of different symmetry, while $\theta_{\bar{\mu}_{01}\bar{\mu}_{1f_i}} < 90^o$ corresponds to transitions between states of the same symmetry.

The dash line in Fig. SI.6 (a) shows the fit obtained employing the Eq. (S.18) with $\theta_{\bar{\mu}_{01}\Delta\bar{\mu}_{01}} = 8^o \pm 4^o$. Such result is in good agreement with one obtained by using the theoretical results of response function calculations ($\theta_{\bar{\mu}_{01}\Delta\bar{\mu}_{01}} = 11.5^o$, solid line in Fig. SI.6 (a)).
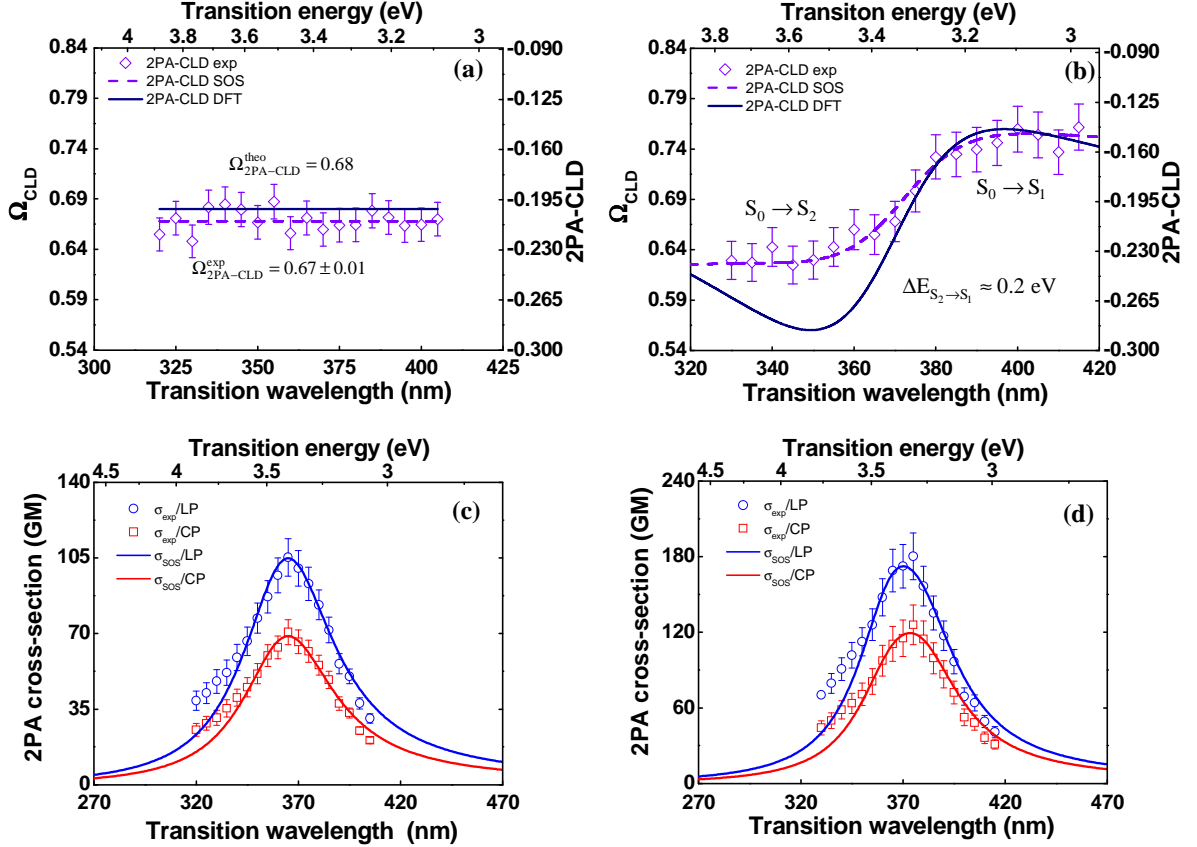

Figure SI.6 – Experimental (diamonds) and simulated (solid lines) 2PA-CLD spectra of (a) **FD43** and (b) **FD48**. Dashed lines show the fit employing the SOS approach. In Fig. SI.6 (c) and (d), the solid lines along the circles and squares correspond to simulated 2PA spectra based on the theoretical results and in Fig. 3 (c) and (d) on the SOS approach.

Following in the same way, the 2PA cross-section for non-centrosymmetric molecules considering a three-energy level system (Fig. SI.6 (b)), can be written as:

$$\sigma_{0\to 2}^{2PA}(\omega) = \frac{2(2\pi)^5}{(nhc)^2}\omega^2 L^4 \left| \sum_{\alpha\beta} \left[\left(\frac{(\hat{e}\bullet\bar{\mu}_{01}^{\alpha\beta})(\bar{\mu}_{12}^{\alpha\beta}\bullet\hat{e})}{\omega_{01}-\omega+i\Gamma_{01}(\omega)} + \frac{(\hat{e}\bullet\bar{\mu}_{02}^{\alpha\beta})(\Delta\bar{\mu}_{02}^{\alpha\beta}\bullet\hat{e})}{\omega} \right) \right] \right|^2 g_{02}(2\omega). \qquad (S.19)$$

Calculating the square modules, we obtained:

$$\sigma_{0\to2}^{2PA}(\omega)=\frac{2(2\pi)^5}{(nhc)^2}L^4\sum_{\alpha\beta}R(\omega)\begin{bmatrix}\left(\hat{e}\cdot\bar{\mu}_{02}^{\alpha\beta}\right)\left(\bar{\mu}_{02}^{\alpha\beta}\cdot\hat{e}\right)^*\left(\Delta\bar{\mu}_{02}^{\alpha\beta}\cdot\hat{e}\right)\left(\hat{e}\cdot\Delta\bar{\mu}_{02}^{\alpha\beta}\right)^*+\\\left(\hat{e}\cdot\bar{\mu}_{01}^{\alpha\beta}\right)\left(\bar{\mu}_{01}^{\alpha\beta}\cdot\hat{e}\right)^*\left(\bar{\mu}_{12}^{\alpha\beta}\cdot\hat{e}\right)\left(\hat{e}\cdot\bar{\mu}_{12}^{\alpha\beta}\right)^*+\\2R(\omega)\frac{(\omega_{01}-\omega)}{\omega}\left(\hat{e}\cdot\bar{\mu}_{01}^{\alpha\beta}\right)\left(\hat{e}\cdot\bar{\mu}_{12}^{\alpha\beta}\right)^*\left(\bar{\mu}_{02}^{\alpha\beta}\cdot\hat{e}\right)^*\left(\Delta\bar{\mu}_{02}^{\alpha\beta}\cdot\hat{e}\right)\end{bmatrix}g_{02}(2\omega),\tag{S.20}$$

where $\bar{\mu}_{12}$ is the transition dipole moment between the two 2PA allowed excited states $(S_1\to S_2)$ and $R(\omega)=\omega^2\big/\left[(\omega_{01}-\omega)^2+\Gamma_{01}^2(\omega)\right]$ is the resonance enhancement factor. Using the Euler integral the 2PA cross-section is given by:

$$\left\langle\sigma_{0\to2}^{2PA}(\theta,\psi,\phi)\right\rangle=\frac{2(2\pi)^5}{(nhc)^2}L^4\frac{1}{8\pi^2}\begin{Bmatrix}\int_0^{2\pi}d\phi\int_0^{2\pi}d\psi\int_0^\pi\sum_{\alpha\beta}\left(\hat{e}\cdot\bar{\mu}_{02}^{\alpha\beta}\right)\left(\bar{\mu}_{02}^{\alpha\beta}\cdot\hat{e}\right)^*\left(\Delta\bar{\mu}_{02}^{\alpha\beta}\cdot\hat{e}\right)\left(\hat{e}\cdot\Delta\bar{\mu}_{02}^{\alpha\beta}\right)^*sen(\theta)d\theta+\\\int_0^{2\pi}d\phi\int_0^{2\pi}d\psi\int_0^\pi\sum_{\alpha\beta}\left(\hat{e}\cdot\bar{\mu}_{01}^{\alpha\beta}\right)\left(\bar{\mu}_{01}^{\alpha\beta}\cdot\hat{e}\right)^*\left(\bar{\mu}_{12}^{\alpha\beta}\cdot\hat{e}\right)\left(\hat{e}\cdot\bar{\mu}_{12}^{\alpha\beta}\right)^*R(\omega)sen(\theta)d\theta+\\\int_0^{2\pi}d\phi\int_0^{2\pi}d\psi\int_0^\pi\sum_{\alpha\beta}2\left(\hat{e}\cdot\bar{\mu}_{01}^{\alpha\beta}\right)\left(\hat{e}\cdot\bar{\mu}_{12}^{\alpha\beta}\right)^*\left(\bar{\mu}_{02}^{\alpha\beta}\cdot\hat{e}\right)^*\left(\Delta\bar{\mu}_{02}^{\alpha\beta}\cdot\hat{e}\right)R(\omega)\frac{(\omega_{01}-\omega)}{\omega}sen(\theta)d\theta\end{Bmatrix}g_{02}(2\omega).\tag{S.21}$$

Considering the linearly and circularly polarized beams and the orientational average methodology described by Andrews and Thirunamachandran [19], the Eq. (S.21) provides the following equation in a three-energy level system for non-centrosymmetric molecules [21]:

$$\sigma_{0\to2}^{2PA}(\omega)=\frac{2}{30}\frac{(2\pi)^5}{(nhc)^2}L^4\begin{bmatrix}P\left(\theta_{\bar{\mu}_{02}\Delta\bar{\mu}_{02}}\right)|\bar{\mu}_{02}|^2|\Delta\bar{\mu}_{02}|^2+\\P\left(\theta_{\bar{\mu}_{01}\bar{\mu}_{12}}\right)R(\omega)|\bar{\mu}_{01}|^2|\bar{\mu}_{12}|^2+\\2P\left(\theta_{\bar{\mu}_{01}\bar{\mu}_{12}\bar{\mu}_{02}\Delta\bar{\mu}_{02}}\right)R(\omega)\frac{(\omega_{01}-\omega)}{\omega}|\bar{\mu}_{01}||\bar{\mu}_{12}||\bar{\mu}_{02}||\Delta\bar{\mu}_{02}|\end{bmatrix}g_{02}(2\omega).\tag{S.22}$$

The polarization parameters ($P(\theta)$) are given by:

$$\kappa=P_L\left(\theta_{\bar{\mu}_{01}\bar{\mu}_{12}}\right)=2\left[2\cos^2\left(\theta_{\bar{\mu}_{01}\bar{\mu}_{12}}\right)+1\right]\tag{S.23}$$

$$\rho=P_L\left(\theta_{\bar{\mu}_{02}\Delta\bar{\mu}_{02}}\right)=2\left[2\cos^2\left(\theta_{\bar{\mu}_{02}\Delta\bar{\mu}_{02}}\right)+1\right]\tag{S.24}$$

$$\varsigma=P_L\left(\theta_{\bar{\mu}_{01}\bar{\mu}_{12}\bar{\mu}_{02}\Delta\bar{\mu}_{02}}\right)=2\begin{bmatrix}\cos\left(\theta_{\bar{\mu}_{02}\Delta\bar{\mu}_{02}}\right)\cos\left(\theta_{\bar{\mu}_{01}\bar{\mu}_{12}}\right)+\\\cos\left(\theta_{\bar{\mu}_{12}\Delta\bar{\mu}_{02}}\right)\cos\left(\theta_{\bar{\mu}_{01}\bar{\mu}_{02}}\right)+\cos\left(\theta_{\bar{\mu}_{01}\Delta\bar{\mu}_{02}}\right)\cos\left(\theta_{\bar{\mu}_{02}\bar{\mu}_{12}}\right)\end{bmatrix}\tag{S.25}$$

for **linear polarization** and

$$\psi=P_C\left(\theta_{\bar{\mu}_{01}\bar{\mu}_{12}}\right)=\left[\cos^2\left(\theta_{\bar{\mu}_{01}\bar{\mu}_{12}}\right)+3\right]\tag{S.26}$$

S.14

$$\zeta = P_C\left(\theta_{\bar{\mu}_{02}\Delta\bar{\mu}_{02}}\right) = \left[\cos^2\left(\theta_{\bar{\mu}_{02}\Delta\bar{\mu}_{02}}\right) + 3\right] \tag{S.27}$$

$$\vartheta = P_C\left(\theta_{\bar{\mu}_{01}\bar{\mu}_{12}\bar{\mu}_{02}\Delta\bar{\mu}_{02}}\right) = \begin{bmatrix} -2\cos\left(\theta_{\bar{\mu}_{02}\Delta\bar{\mu}_{02}}\right)\cos\left(\theta_{\bar{\mu}_{01}\bar{\mu}_{12}}\right) + \\ 3\cos\left(\theta_{\bar{\mu}_{12}\Delta\bar{\mu}_{02}}\right)\cos\left(\theta_{\bar{\mu}_{01}\bar{\mu}_{02}}\right) + 3\cos\left(\theta_{\bar{\mu}_{01}\Delta\bar{\mu}_{02}}\right)\cos\left(\theta_{\bar{\mu}_{02}\bar{\mu}_{12}}\right) \end{bmatrix} \tag{S.28}$$

for **circular polarization**.

The Eq. (S.22) describes the 2PA cross-section from ground to the second excited state ($\sigma_{02}^{(2PA)}(\omega)$) with an intermediate energy level (S_1). Therefore, in a three-energy level system (Fig. SI.5 (b)), the 2PA cross-section is governed by three contributions: the first corresponds to a 2PA transition in a two-level system with a change of permanent dipole moment ($\Delta\bar{\mu}_{02} \neq 0$), while the second contribution corresponds to transitions in a three-energy level system with one final excited state (S_2) and one intermediate real excited state (S_1) which is responsible by the resonance enhancement of the nonlinearity. The last contribution corresponds to interference between the two excitation pathways previously described. However, if the excitation photon energy is very close to the intermediate real state ($\omega \rightarrow \omega_{01}$), the contribution of the interference term to the total 2PA cross-section is very small. Otherwise, if the two excited states are very close the interference term can strongly increase or decrease the 2PA cross-section, depending on the relative phase between the dipole moments.

Since, according to the theoretical calculations, the **FD48** molecule presents two 2PA allowed transitions very close in energy and with similar 2PA probabilities ($\bar{\delta}_{S_0 \rightarrow S_1}^{2PA} = 53500$ a.u. and $\bar{\delta}_{S_0 \rightarrow S_2}^{2PA} = 50800$ a.u.), it is necessary to consider a two plus three-energy level diagram in this case. The diagram shown in Fig. SI.5 (c) refers to the two plus three-energy level diagram which is a linear combination of the two diagrams previously reported. In this system the Ω_{CLD}^{2PA} signal can be written as

$$\Omega_{CLD}^{2PA}(\omega) = \frac{\sigma_{2PA}^{PC}}{\sigma_{2PA}^{PL}} = \frac{\alpha\eta g_{01}(2\omega) + \left[\beta\kappa + R(\omega)\chi\rho + 2R(\omega)\gamma\dfrac{(\omega_{01}-\omega)}{\omega}\varsigma\right]g_{02}(2\omega)}{\alpha\tau g_{01}(2\omega) + \left[\beta\psi + R(\omega)\chi\zeta + 2R(\omega)\gamma\dfrac{(\omega_{01}-\omega)}{\omega}\vartheta\right]g_{02}(2\omega)}, \tag{S.29}$$

with

$$\alpha = \left|\vec{\mu}_{01}\right|^2 \left|\Delta\vec{\mu}_{01}\right|^2 = \frac{3\times10^3 \ln(10)(hc)^2}{(2\pi)^2 N_A} \frac{n}{L^2} \frac{\varepsilon(\omega_{01})}{\omega_{01} g_{max}(\omega_{01})} \frac{\partial \tilde{\upsilon}}{\partial F} a^3, \tag{S.30}$$

$$\beta = \left|\vec{\mu}_{02}\right|^2 \left|\Delta\vec{\mu}_{02}\right|^2 = \frac{3\times10^3 \ln(10)(hc)^2}{(2\pi)^2 N_A} \frac{n}{L^2} \frac{\varepsilon(\omega_{02})}{\omega_{02} g_{max}(\omega_{02})} \frac{\partial \tilde{\upsilon}}{\partial F} a^3, \tag{S.31}$$

$$\chi = \left|\vec{\mu}_{01}\right|^2 \left|\vec{\mu}_{12}\right|^2 = \left[\frac{3\times10^3 \ln(10)(hc)^2}{(2\pi)^2 N_A} \frac{n}{L^2}\right]^2 \frac{\varepsilon(\omega_{01})}{g_{max}(\omega_{01})\omega_{01}} \frac{\varepsilon(\omega_{12})}{g_{max}(\omega_{02})\omega_{12}}, \tag{S.32}$$

$$\gamma = \left|\vec{\mu}_{01}\right|\left|\vec{\mu}_{12}\right|\left|\vec{\mu}_{02}\right|\left|\Delta\vec{\mu}_{02}\right| = \sqrt{BC}, \tag{S.33}$$

where $\varepsilon(\omega_{g\rightarrow f})$ is the peak molar absorptivity corresponding at maximum transition frequency $\omega_{g\rightarrow f}$ and N_A is the Avogadro's number. $\tilde{\upsilon} = \tilde{\upsilon}_{abs} - \tilde{\upsilon}_{em}$ is the difference between the wavenumber of the fluorescence and absorption spectrum maxima (in cm^{-1}). $F(n,\xi) = 2(\xi-1)/(2\xi+1) - 2(n^2-1)/(2n^2+1)$ is the Onsager polarity function with ξ being the dielectric constant of the solvent. a is the radius of the molecular cavity, assumed as spherical. The parameters α, β, χ and γ can be obtained through of solvatochromic shift measurements as reported in Ref. [1]. The other parameters ($\eta, \kappa, \rho, \varsigma, \tau, \psi, \zeta$ and ϑ) are given by the Eqs. (S.16-17) and (S.23-28). To obtain the angle between the dipole moments from experimental data we modeled the experimental 2PA-CLD spectrum (dash line in Fig. SI.6 (b)) using the least square-based finite difference method [23] taken as initial values those obtained through the theoretical calculations.

It is important to mention that the angles set used to model the 2PA-CLD spectrum should necessarily fit the 2PA spectra obtained using both linearly and circularly polarized light (solid lines in Figs. SI.6 (c) and SI.6 (d)). It is observed that, in general, there is good agreement between the experimental data and theoretical results. The values estimated for the parameter B and the angle between the dipole moments $\vec{\mu}_{01}$ and $\Delta\vec{\mu}_{01}$ are the only exceptions, in those cases a considerable difference is observed. These parameters, to some extent, may explain the difference between the experimental and theoretical data verified in Fig. SI.6 (b) for the spectral region below 360 nm.

Table SI.2 – Estimates of the angles between the dipole moments of FD48 molecule. The estimates were made based on the theoretical results (DFT) and by modeling the experimental 2PA-CLD spectrum using the sum-over-essential states (SOS) approach.

Dipole angles	DFT	SOS
$\theta_{\vec{\mu}_{01}\Delta\vec{\mu}_{01}}$	18°	45°
$\theta_{\vec{\mu}_{02}\Delta\vec{\mu}_{02}}$	172°	180°
$\theta_{\vec{\mu}_{01}\vec{\mu}_{02}}$	101°	91°
$\theta_{\vec{\mu}_{01}\vec{\mu}_{12}}$	151°	155°
$\theta_{\vec{\mu}_{01}\Delta\vec{\mu}_{02}}$	87°	85°
$\theta_{\vec{\mu}_{02}\vec{\mu}_{12}}$	64°	80°
$\theta_{\vec{\mu}_{12}\Delta\vec{\mu}_{02}}$	108°	118°

SI.4 Sum-over-essential states approach: Two-photon circular dichroism

Two-photon circular dichroism (2PA-CD) is a specific nonlinear optical property for optically active samples because it depends directly on the magnetic transition dipole moment and the electric transition quadrupole moment [20,24]. Basically, the 2PA-CD is defined analogously to the electronic CD widely employed to investigate the secondary structure of proteins, i.e.:

$$\Delta\sigma_{2PA}^{CD}(\omega) = \sigma_L^{2PA}(\omega) - \sigma_R^{2PA}(\omega), \tag{S.34}$$

where $\sigma_L^{2PA}(\omega)$ and $\sigma_R^{2PA}(\omega)$ are the 2PA cross-sections for left and right circularly polarized light.

Normally, the electric dipole terms dominate the nonlinear optical effects, and the magnetic dipole and electric quadrupole contributions may only be measured/identified if the effects of the electric dipole term vanish or they cancel, as is the case in nonlinear circular dichroism.

We performed measurements of the 2PA-CD for both molecules and the results are shown in Fig. SI.7. However, we did not observe, within our experimental error, differences between 2PA using right and left circularly polarized light.
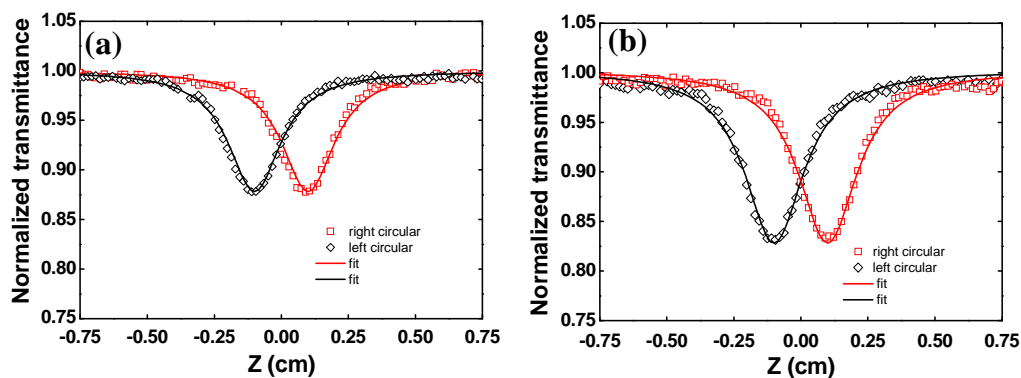

Figure SI.7 – Z-scan curves to the molecules **FD43 and FD48** employing linearly and circularly polarization light. The solid lines represent the fitting. The Z-scan curves (right and left circular polarization) were shifted from the focal position for a better comparison between them.

To obtain an estimative about the magnetic dipole and electric quadrupole contributions to the total 2PA cross-section, we used the differential two-photon absorption

model proposed by Meath [25]. According this model, considering a two- level system, the two-photon circular dichroism can be expressed by:

$$\Delta\sigma_{2PA}^{CD}(\omega) = \sigma_L^{2PA}(\omega) - \sigma_R^{2PA}(\omega) = \sigma_{\bar{m}}^{2PA}(\omega) + \sigma_{\bar{Q}}^{2PA}(\omega),$$ (S.35)

where

$$\sigma_{\bar{m}}^{2PA}(\omega) = \frac{2}{15}\frac{(2\pi)^5}{(nhc)^2}L^4\left\{6|\Delta\vec{\mu}_{01}|^2\left[\text{Im}(\vec{\mu}_{01}\bullet\vec{m}_{01})\right] + 2\vec{\mu}_{01}\bullet\Delta\vec{\mu}_{01}\left[\text{Im}(\vec{m}_{01}\bullet\Delta\vec{\mu}_{01})\right]\right\}$$ (S.36)

and

$$\sigma_{\bar{Q}}^{2PA}(\omega) = \frac{2}{15}\frac{(2\pi)^5}{(nhc)^2}L^4\left\{\frac{\omega}{c}|\Delta\vec{\mu}_{01}|\left[(\vec{\mu}_{01}\times\Delta\vec{\mu}_{01})\bullet\vec{Q}_{01}\right]\right\}.$$ (S.37)

$\sigma_{\bar{m}}^{2PA}(\omega)$ and $\sigma_{\bar{Q}}^{2PA}(\omega)$ are the magnetic and electric quadrupole contributions, respectively. As it can be seen in Eqs. (S.36) and (S.37) the 2PA-CD signal, in a two-level system, depends on the transition dipole moment ($\vec{\mu}_{01}$), the permanent dipole moment change ($\Delta\vec{\mu}_{01}$), the magnetic dipole moment ($\vec{m}_{01}$) and the electric quadrupole moment ($\vec{Q}_{01}$). The two first can be obtained from solvatochromic measurements as previously mentioned. The magnetic dipole moment can be estimated from the conventional CD measurements as reported in the section SI.1. The magnitude of the electric quadrupole moment were estimated through DFT calculations (B3LYP/6-31+G(d)) carried out using the Gaussian 03 package.[7] In this context, we used these parameters and, considering the maximum values from Eqs. (S.36) and (S.37), estimated the 2PA-CD for both molecules. Table SI.3 shows the results obtained to the dipole and quadrupole moments as well as the 2PA-CD signal.

The 2PA-CD signal presented by the **FD43** and **FD48** molecules are 1000 times smaller than their 2PA-CLD signal. Therefore, the 2PA cross-section reported here to the 2PA-CD signal corresponds to a normalized transmittance difference of *c.a.* 0.001, which limited our experimental measurements. It is important to mention that the results presented here to the 2PA-CD based on Meath's Theory are in good agreement with those obtained by Rizzo et. al. [26-30] for molecules with different types of chirality using modern analytical function, within the TD-DFT framework.

Table SI.3 – Magnitude of the dipole and quadrupole moments, as well as the 2PA-CD signal, as determined from the experimental measurements and theoretical calculations.

Molecules	$\left|\vec{\mu}_{01}\right|$	$\left|\Delta\vec{\mu}_{01}\right|$	$\left|\vec{m}_{01}\right|$	$\left|\vec{Q}_{01}\right|$	$\Delta\sigma_{2PA}^{CD}$
FD43	8.5	13.0	1.8×10^{-3}	240	0.014
FD48	8.5	14.5	3.3×10^{-3}	410	0.060

Obs: $\left|\vec{\mu}_{01}\right|$ and $\left|\Delta\vec{\mu}_{01}\right|$ are given in Debye; $\left|\vec{m}_{01}\right|$ is given in Bohr magneton units ($\mu_B = e\hbar/2mc$), $\left|\vec{Q}_{01}\right|$ is given in $Debye \times \AA$ and $\Delta\sigma_{2PA}^{CD}$ in GM.

SI.5 – References

(1) Vivas, M. G.; Silva, D. L.; De Boni, L.; Bretonniere, Y.; Andraud, C.; Laibe-Darbour, F.; Mulatier, J. C.; Zalesny, R.; Bartkowiak, W.; Canuto, S.; Mendonca, C. R. Experimental and Theoretical Study on the One- and Two-Photon Absorption Properties of Novel Organic Molecules Based on Phenylacetylene and Azoaromatic Moieties *Journal of Physical Chemistry B* **2012**, *116*, 14677-14688.

(2) Zhu, L. Y.; Yi, Y. P.; Shuai, Z. G.; Bredas, J. L.; Beljonne, D.; Zojer, E. Structure-property relationships for three-photon absorption in stilbene-based dipolar and quadrupolar chromophores *Journal of Chemical Physics* **2006**, *125*.

(3) Correa, D. S.; De Boni, L.; Misoguti, L.; Cohanoschi, I.; Hernandez, F. E.; Mendonca, C. R. Z-scan theoretical analysis for three-, four- and five-photon absorption *Optics Communications* **2007**, *277*, 440-445.

(4) Becke, A. D. Density-functional thermochemistry. III. The role of exact exchange *The Journal of Chemical Physics* **1993**, *98*, 5648-5652.

(5) Lee, C. T.; Yang, W. T.; Parr, R. G. Development of the colle-salvetti correlation-energy formula into a functional of the electron-density *Physical Review B* **1988**, *37*, 785-789.

(6) Frisch, M. J.; Pople, J. A.; Binkley, J. S. Self-consistent molecular-orbital methods 25. Supplementary functions for Gaussian basis sets *The Journal of Chemical Physics* **1984**, *80*, 3265-3269.

(7) Gaussian03, M. J. Frisch, G.W.T., H. B. Schlegel, G. E. Scuseria, M. A. Robb, J. R. Cheeseman, J. A. Montgomery, Jr., T. Vreven, K. N. Kudin, J. C. Burant, J. M. Millam, et.al., Gaussian Inc., Pittsburgh PA (2003).

(8) DALTON. , a molecular electronic structure program, Release 2.0 (2005), see http://www.kjemi.uio.no/software/dalton/dalton.html, 2005.

(9) McClain, W. M. Excited State Symmetry Assignment through Polarized 2-Photon Absorption Studies of Fluids *The Journal of Chemical Physics* **1971**, *55*, 2789-2796.

(10) Silva, D. L.; Murugan, N. A.; Kongsted, J.; Rinkevicius, Z.; Canuto, S.; Ågren, H. The Role of Molecular Conformation and Polarizable Embedding for One- and Two-Photon Absorption of Disperse Orange 3 in Solution *The journal of physical chemistry B* **2012**, *116*, 8169–8181.

(11) Vivas, M. G.; Silva, D. L.; De Boni, L.; Zalesny, R.; Bartkowiak, W.; Mendonca, C. R. Two-photon absorption spectra of carotenoids compounds *Journal of Applied Physics* **2011**, *109*, 103529-103521 - 103529-103528.

(12) Toro, C.; De Boni, L.; Lin, N.; Santoro, F.; Rizzo, A.; Hernandez, F. E. Two-Photon Absorption Circular-Linear Dichroism on Axial Enantiomers *Chirality* **2010**, *22*, E202-E210.

(13) Toro, C.; De Boni, L.; Lin, N.; Santoro, F.; Rizzo, A.; Hernandez, F. E. Two-Photon Absorption Circular Dichroism: A New Twist in Nonlinear Spectroscopy *Chemistry-a European Journal* **2010**, *16*, 3504-3509.

(14) Vivas, M. G.; Dias, C.; Echevarría, L.; Mendonca, C. R.; Hernandez, F. E.; De Boni, L. Two-Photon Circular-Linear Dichroism of Perylene in Solution: A Theoretical-Experimental Study *The journal of physical Chemistry B* **2013**.

(15) Wanapun, D.; Wampler, R. D.; Begue, N. J.; Simpson, G. J. Polarization-dependent two-photon absorption for the determination of protein secondary structure: A theoretical study *Chemical Physics Letters* **2008**, *455*, 6-12.

(16) Drobizhev, M.; Makarov, N. S.; Tillo, S. E.; Hughes, T. E.; Rebane, A. Two-photon absorption properties of fluorescent proteins *Nature Methods* **2011**, *8*, 393-399.

(17) Bonin, K. D.; McIlrath, T. J. Two-photon electric-dipole selection rules *Journal of the Optical Society of American B* **1984**, *1*, 52-55.

(18) Nascimento, M. A. C. The polarization dependence of 2-photon absorption rates for randomly oriented molecules *Chemical Physics* **1983**, *74*, 51-66.

(19) Andrews, D. L.; Thirunamachandran, T. On three-dimensional rotational averages *Journal of Chemical Physics* **1977**, *67*, 5026.

(20) Power, E. A.; Thirunamachandran, T. Circular dichroism: A general theory based on quantum electrodynamics *Journal of Chemical Physics* **1974**, *60*, 3695.

(21) Meath, W. J.; Power, E. A. On the importance of permanent moments in multiphoton absorption using perturbation-theory *Journal of Physics B-Atomic Molecular and Optical Physics* **1984**, *17*, 763-781.

(22) Kamada, K.; Ohta, K.; Iwase, Y.; Kondo, K. Two-photon absorption properties of symmetric substituted diacetylene: drastic enhancement of the cross section near the one-photon absorption peak *Chemical Physics Letters* **2003**, *372*, 386-393.

(23) Nielsen, K. L. *Methods in Numerical Analysis* Macmillan: New York, 1966.

(24) Tinoco, I. Two-photon circular dichroism *Journal Chemical Physics* **1975**, *62* 1006-1009.

(25) Meath, W. J.; Power, E. A. Differential multiphoton absorption by chiral molecules and the effect of permanent moments *Journal of Physics B-Atomic Molecular and Optical Physics* **1987**, *20*, 1945-1964.

(26) Guillaume, M.; Ruud, K.; Rizzo, A.; Monti, S.; Lin, Z.; Xu, X. Computational Study of the One- and Two-Photon Absorption and Circular Dichroism of (L)-Tryptophan *Journal of Physical Chemistry B* **2010**, *114*, 6500-6512.

(27) Jansik, B.; Rizzo, A.; Agren, H. Ab initio study of the two-photon circular dichroism in chiral natural amino acids (vol 111B, pg 2409, 2007) *Journal of Physical Chemistry B* **2007**, *111*, 2409-2414.

(28) Jansik, B.; Rizzo, A.; Agren, H.; Champagne, B. Strong two-photon circular dichroism in helicenes: A theoretical investigation *Journal of Chemical Theory and Computation* **2008**, *4*, 457-467.

(29) Rizzo, A. Recent progress in the computation of non linear optical properties of chiral systems. In *Computational Methods in Science and Engineering Vol 1 - Theory and Computation: Old Problems and New Challenges*; Maroulis, G., Simos, T. E., Eds., 2007; Vol. 963; pp 379-388.

(30) Diaz, C.; Lin, N.; Toro, C.; Passier, R.; Rizzo, A.; Hernandez, F. E. The Effect of the pi-Electron Delocalization Curvature on the Two-Photon Circular Dichroism of Molecules with Axial Chirality *Journal of Physical Chemistry Letters* **2012**, *3*, 1808-1813.